

Article

Comparison of Different Grid Cell Ordering Approaches in a Simplified Inundation Model

Tsun-Hua Yang ¹, Yi-Chin Chen ^{2,*}, Ya-Chi Chang ^{1,†}, Sheng-Chi Yang ^{1,†}
and Jui-Yi Ho ^{1,†}

¹ Hydrotech Division, Taiwan Typhoon and Flood Research Institute, National Applied Research Laboratories, 11F., No. 97, Sec. 1, Roosevelt Rd., Taipei City 10093, Taiwan; E-Mails: tshyang@narlabs.org.tw (T.-H.Y.); rachel-chang@narlabs.org.tw (Y.-C.C.); shirky@narlabs.org.tw (S.-C.Y.); juiyiho@narlabs.org.tw (J.-Y.H.)

² Department of Geography, National Changhua University of Education, No. 1, Jinde Rd., Changhua City, Changhua County 50007, Taiwan

† These authors contributed equally to this work.

* Author to whom correspondence should be addressed; E-Mail: yichinchen@cc.ncue.edu.tw; Tel.: +886-4-7232105; Fax: +886-4-7211186.

Academic Editor: Miklas Scholz

Received: 1 December 2014 / Accepted: 22 January 2015 / Published: 30 January 2015

Abstract: This study proposes a simplified model for non-riverine flood routing using a digital elevation model. The model has the advantage of running with only a few types of input, such as topographic data and cumulative rainfall. Given its ease of use, the model is stable and reliable for developing a real-time inundation forecasting system. This model uses two approaches to determine the collection of cells from which flooding is assumed to originate: (1) A traditional “lowest-elevation approach” that assumes flooding originates from the lowest elevations and that is only based on topographic data; and (2) a novel “D-infinity contributing area approach” that assumes flooding originates at the cells toward which the flow moves and that considers *in situ* topography and upslope information. The flood water is transferred based on the flat-water assumption that the water levels of adjacent cells are equalized. The performance was evaluated by comparing the simulated results with those from a complex inundation model. The simplified model with the lowest elevation assumption has limited applicability in flat areas and did not provide reasonable locations of the source of

the flood. The D-infinity approach can improve the simplified inundation model and extend its application in various topographical areas.

Keywords: flooding; simplified inundation model; flat-water assumption, D-infinity contributing area

1. Introduction

Flooding is a major natural hazard. Once floods occur, the casualties and financial losses for highly populated areas are inevitably large (e.g., [1–3]). Flooding is generally a function of river overflows, storm surges, and intense rainfall. Thus, strategies to mitigate flooding hazards include structural measures, such as detention basins and levee projects, and non-structural measures, such as floodplain regulations, emergency preparedness, and early warning systems [4]. A robust and reliable model is necessary to predict the effect of flooding and to implement appropriate strategies [5].

Several studies have developed simplified flood inundation models [4,6–12] to simulate potential flood areas. These models are based on the digital elevation model (DEM) and use a simple set of rules to simulate the spread of flood water over a given area. As a consequence, the models require less computational resources than complex two-dimensional (2-D) inundation models (e.g., WASH-123D [13,14] and FLO-2D [15]) and may be more practical for real-time warnings. These complex models consider detailed hydraulic processes by solving complicated governing equations (e.g., Saint Venant equations) that are computationally intensive [16]. Several studies used adaptive grids, parallel computing, or Graphics Processing Units (GPUs) to accelerate computer speed at real-time level (e.g., [17,18]). To develop a high-performance real-time forecasting system by using these complex models, however, requires higher hardware resources and technical skill. Therefore, the development of simplified and cost-effective models (e.g., [6,8,10–12,19]) is still a topic of interest. Lhomme *et al.* [7] developed a simplified hydraulic model (the rapid flood spreading method, RFSM) to maintain model runtimes at practical levels. The concept behind the RFSM is to spread the total flood volume in floodplain areas over the floodplain by considering the topography. Zerger *et al.* [4] used a flat-water assumption model to simulate coastal storm-surge risk for the coastal community of Cairns, Australia. The flat-water assumption involves distributing water between cells and their neighboring cells until the water levels are equal. Moreover, Chen *et al.* [19] used a flat-water model to simulate non-riverine, urban flooding on the campus of the University of Memphis, Tennessee. The authors noted that a traditional approach to apply a flat-water model is to determine route starting cells, which are a collection of cells from which flooding is assumed to originate, from the lowest elevation. Rather than the traditional approach, they used a collection of route starting cells based on the highest one percent of the flow accumulation values. However, the details regarding the selection process of routing start points were not addressed in the study.

The studies noted above assumed that water spreads from the lowest elevation locations in a given area to determine the route starting cells. However, the assumption that water spreads from the lowest elevation area may oversimplify the effect of topography on flooding. This assumption may only be applicable in flat floodplain areas. In hilly areas, the runoff water is accumulated in a local depression or channel. Soulis [20] considered the flow direction and accumulation to the DEM-based hydrological

models. He concluded that it can be applied in arbitrarily shaped areas and not strictly in the limits of specific watershed. This study thus applies the flow direction and accumulation to identify the route starting cells. These ordered cells can be used to improve the performance of simplified inundation models.

In this study, a simplified inundation model (hereafter called SPM) using the flat-water assumption is proposed. A collection of route starting cells is identified using two different grid cell ordering approaches: (1) A traditional approach using the lowest elevation assumption (hereafter called SPM_E), which is based on topographic data; and (2) a novel approach using the D-infinity (means an infinite number of possible single flow directions) contributing area assumption, which is based on the amount of flow into a cell (hereafter called SPM_D). The highest values of flow accumulation are then selected as the route starting cells. The two approaches were compared. Because the historical data are insufficient for meaningful comparisons, the same simulations performed by WASH123D were used as a benchmark to evaluate the performance of the SPM. Application of the SPM to three towns that are subject to flooding in Pingtung County demonstrates the method's effectiveness and applicability in flood prone areas.

2. Methods

The data processing and modeling flowchart of the SPM is shown in Figure 1. The model used a gridded DEM to determine the route starting cells and the distribution of flood water. The route starting cells were chosen according to either the D-infinity contributing area or topographic elevation. Each cell has a calculated contributing area and an elevation. The model sorts all cells based on the contributing area in a descending order or based on the elevation in an ascending order. Flood water starts filling in a collection of route starting cells in an incremental interval from the first i th percent of the lowest elevation or of the highest contributing area. The i is an empirical number. When the level at any starting cell is higher than the surrounding cells, the flood water spreads to the neighboring cells based on the flat-water assumption. The process of water filling and dispersing stops, and the results are the output when all of the water is assigned. Details regarding each approach used in the model are described as follows.

2.1. D-Infinity Contributing Area Approach

To determine the start routing cells, we calculate the flow accumulation area for each cell by using the D-infinity method. D-infinity is a method for identifying the flow direction and contributing areas in gridded DEMs proposed by Tarboton [21]. This method is better for determining flow accumulation compared with the traditional D8 method, a single flow direction method assigns flow from each grid cell to one of eight neighbors.

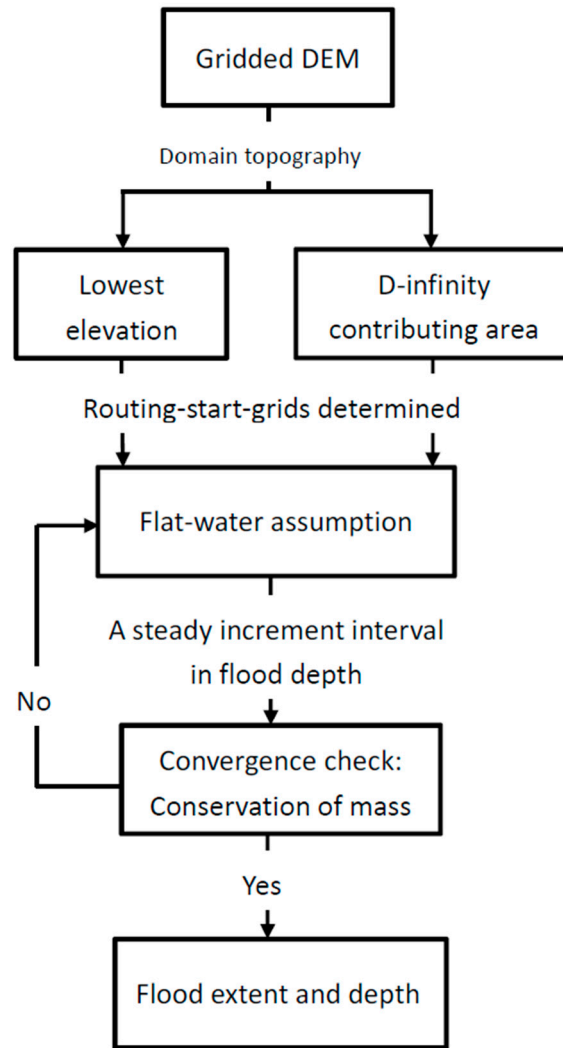


Figure 1. Overview of simplified inundation model (SPM) calculating process. (DEM—digital elevation model).

The flowchart and pseudo code for the D-infinity contributing area are shown in Figure 2. Before calculating the flow direction, a standard pre-processed algorithm for sink fill is applied to remove the depressions by using the fill function in ESRI ArcGIS. These are the areas surrounded by higher elevation values in the gridded DEM [22]. Then, the angle of the flow direction of a cell is determined as the steepest downward slope from all eight facets (Figure 3a). Calculation of slope on a single facet is based on the differences in elevation between the neighbor's cells (Figure 3b). If the direction falls between two adjacent neighbors (*i.e.*, the direction in Figure 3a), then the flow is portioned between these two cells according to the flow direction angles $\alpha_1/(\alpha_1 + \alpha_2)$ and $\alpha_2/(\alpha_1 + \alpha_2)$. If the flow is directed at an adjacent neighbor (e.g., the directional angles are 0, $\pi/4$, $\pi/2$, $3\pi/4$, π , $5\pi/4$, $3\pi/2$ and $7\pi/4$), then the flow drains to one neighboring cell. By using the flow direction algorithm, the flow contributing area is calculated based on the number of cells flowing into each cell. All of the cells can then be rearranged in a sequence of descending contributions from high to low. The cells with higher contributing areas tend to be located downstream and have a greater upslope runoff contribution. Therefore, these cells are assumed to have a higher risk of flooding.

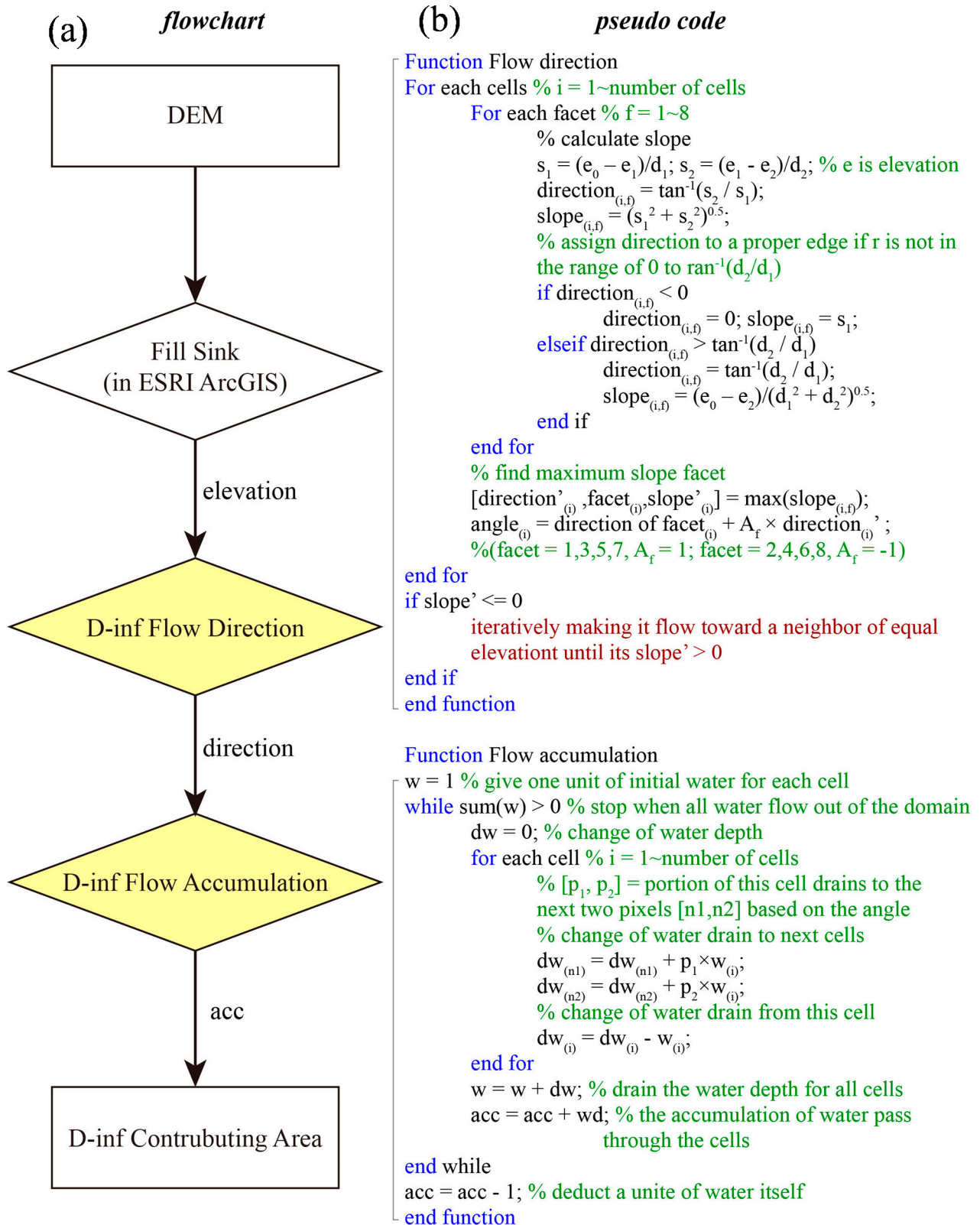


Figure 2. Flowchart and pseudo code for D-infinity contributing area: (a) The chart shows the pseudo codes of D-inf flow direction and D-inf flow accumulation (yellow rhombus in the flowchart); (b) The blue code is for loop or if statement; green is comment; red is an iteratively function.

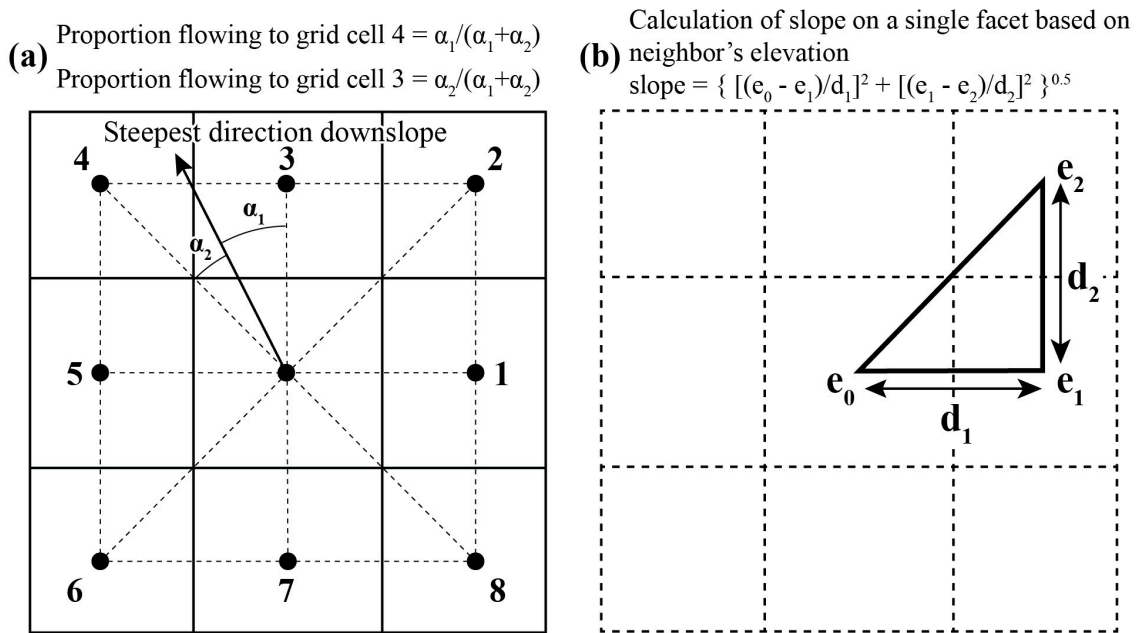


Figure 3. Flow direction using the D-infinity flow model (redrawn from [21]): (a) shows proportion of water flowing into two adjacent cells; and (b) shows calculation of slope on a single facet.

2.2. Lowest Elevation Approach

The lowest elevation approach assumes that water fills from the cells with the lowest elevation, as predetermined from topographic data. The cells with the lowest elevation, also known as depressions [23], are areas surrounded by higher terrain and have no outlet to lower areas. Naturally, these are the spots where flood water begins to accumulate. Several studies, such as [19,24], routed water from the lowest spots. While preprocessing the DEM, the orders of all cells are reorganized from lowest to highest based on topographical data. Consistent with the D-infinity approach, the top one percent of the sequence was selected to start the flood water accumulation.

2.3. Flat-Water Assumption

A flat-water inundation model was developed in which the water spreads from multiple route starting cells. The model only requires the input of a water volume, boundary information, and a DEM. The flat-water assumption can be used in situations where a paucity of detailed hydraulic and hydrological data makes more complex models impractical [10]. The flood water volume input was calculated by multiplying the total efficient rainfall (I) by the domain area (A). Water loss is ignored, and the total volume of rainfall and surface runoff are alternative terms that reference the total volume of flood water in this study. The equation is expressed as:

$$\text{Total Flood Volume} = \sum_{i=1}^n I \times A \tag{1}$$

Figure 4 presents an example of water spreading. The water initially accumulates at the route starting cells (e.g., Z_1 in Figure 4a) in increments. As noted earlier, this study used two approaches, *i.e.*, the

highest flow accumulation and lowest elevation approaches, to select the cells. An incremental water depth is continually added to the cells until the difference between the water volume in the modeling domain and the input volume is less than 10%. The Z_1 cell is labeled as a wet cell, and its surrounding cells are labeled as dry cells. The water level is increased until the water spreading condition $Z_1 + \Delta h_1 > Z_2$ is met (Figure 4b). By adding water, the (Z_2) cell switches from a dry cell to a wet cell. The added depth Δh_2 should meet the flat water assumption of $Z_1 + \Delta h_1 = Z_2 + \Delta h_2$ (Figure 4c). All of the wet cells in the modeling domain are added in increments, and the neighboring cells are examined to determine whether the flat-water assumption is met.

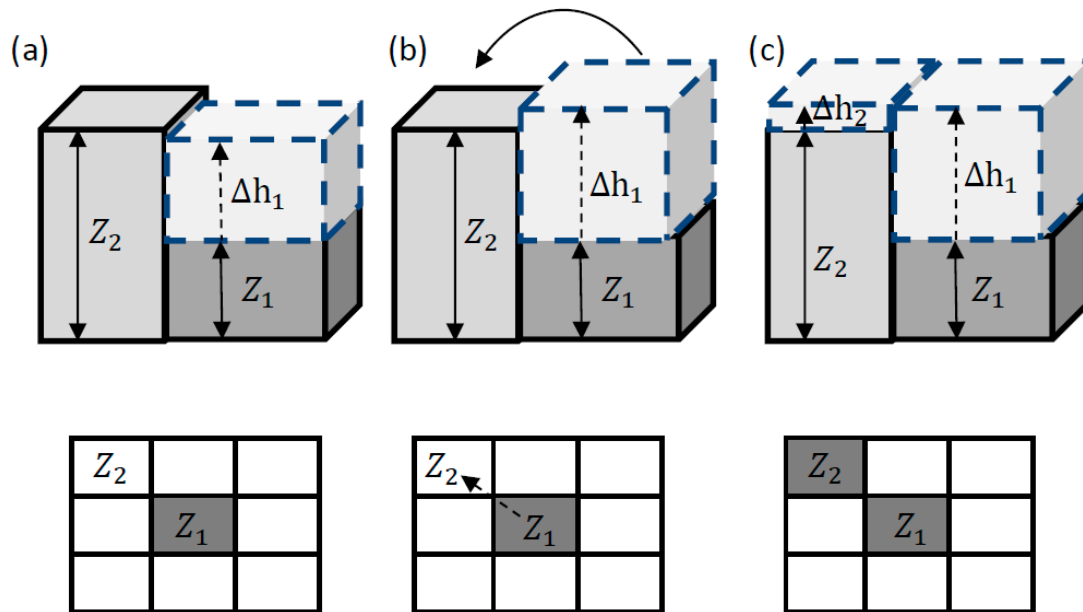


Figure 4. Water spreading using the flat-water assumption in the simplified inundation model: (a) A flood occurs at cell Z_1 ; (b) Flood water over flows to cell Z_2 ; and (c) The water surface at cells Z_1 and Z_2 are equivalent.

In addition, the increment interval can affect the modeling results in terms of conservation of mass [4,19]. Chen *et al.* [19] applied a DEM with $10\text{ m} \times 10\text{ m}$ resolution and demonstrated that the results change slightly once increment intervals are equal to or less than 0.01 m. Given different topographic information, the ideal increment value may change. This study considered topographies similar to Chen *et al.* [19]; thus, an increment of 0.01 m is sufficiently small to achieve convergence.

3. Model Validation

3.1. Case Study

The application of the proposed model is validated using examples of three towns (Figure 5) in Pingtung County, Taiwan, where flood hazards occur frequently during the typhoon season (May to October). The three towns are Pingtung, Linbian, and Hengchuen, which are characterized by different topographies. The topographies in Pingtung and Linbian are both alluvial plains with low reliefs and elevations. Groundwater overdraft causes land subsidence, stopping rainfall water from gravity draining effectively and increasing flood damage in Linbian. From the topographic maps derived from a

40 m \times 40 m DEM (Figure 5), obvious artificial drainage channels are found in Pingtung but not in Linbian. Compared to the flat areas, the topography in Hengchuen is mainly composed of a rift valley in the north, flat areas and low elevations in the center and hills in the surrounding areas. The applications in these regions can help test the model performance in different topographies.

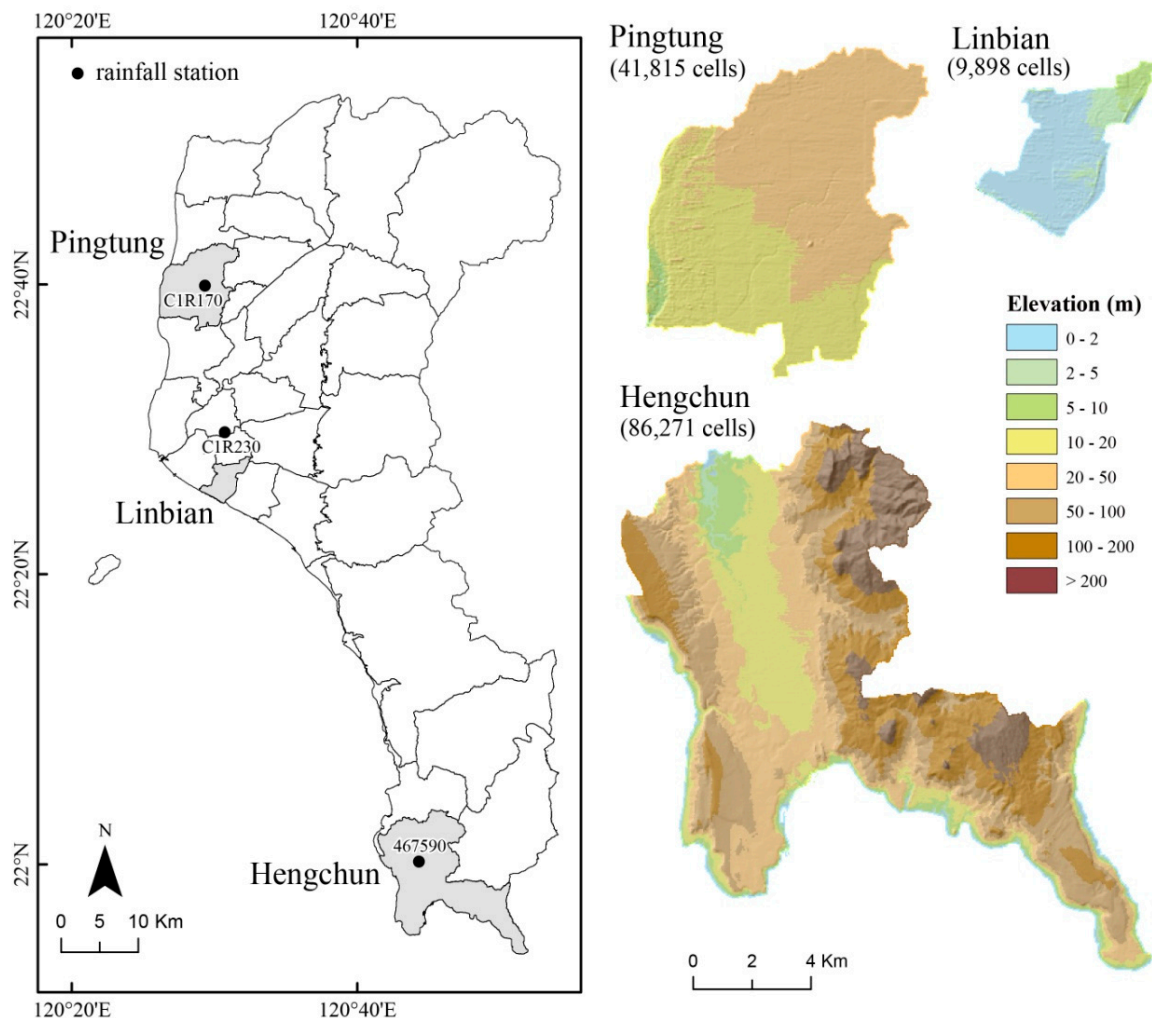


Figure 5. Map of Pingtung County and three selected towns, Pingtung, Linbian, and Hengchun.

The 40 m \times 40 m DEMs were used to implement the SPM. There are 41,815 cells in Pingtung, 9898 cells in Linbian, and 86,271 cells in Hengchuen. 1% of the cells was assumed as route starting cells. There were 418, 98 and 862 cells for Pingtung, Linbian and Hengchuen, respectively. Considering rainfall from extreme events, the observed rainfall during typhoons was used as the model input. Accumulated rainfall values of 730, 401 and 615 mm over 24 h were recorded at the C1R170, C1R230, and 46,750 stations (Figure 5) in Pingtung, Linbian, and Hengchuen, respectively.

3.2. Validation of the Model Performance

To validate the model performance, the 2-D hydraulic model, WASH123D was used to simulate the flood areas of the three towns based on the same initial conditions. WASH123D provides many robust options for solving overland flow equations, and it can be applied in a wide range of application-dependent circumstances [13]. Additional details can be obtained from Yeh *et al.* [25,26]. In

this study, the particle-tracking approach is utilized to solve the diffusion wave equations in this time varying model. Rainfall hydrographs are used as the only input information, since the infiltration, evapotranspiration and other artificial sources/sinks are neglected in this study. Roughness coefficient of the land surface is the main parameter in this model. Water depth on the boundary is assumed to be zero. By comparing the WASH123D and SPM simulations, the performances regarding the accuracy and computation time are evaluated to determine whether the simplified model can serve as an alternative for complex inundation models. On the other hand, the inundation area data in Pingtung during Typhoon Fanapi in 2010 and in Hengchun during Typhoon Nanmadol in 2011 was used to compare with the simulated results. The data was collected from National Pingtung University of Science and Technology, Pingtung city, Taiwan. The inundation areas were identified and mapped by field survey.

A fit indicator [6,7,11] for evaluating the model performance is defined as follows:

$$Fit = \frac{\text{Overlapped Flooded Area}}{\text{Total Flooded Area}} = \frac{\text{Flooded Area}_{SPM} \cap \text{Flooded Area}_{WASH123D}}{\text{Flooded Area}_{SPM} \cup \text{Flooded Area}_{WASH123D}} \quad (2)$$

The total flooded area was calculated by the union of the SPM and WASH123D forecasts. The overlapping flood area is the interaction of these two models. The value of the indicator is between 0.0 and 1.0; a higher value represents a better performance. Residential and non-residential properties, people, and critical services are typically vulnerable to a flood depth of 0.3 m or greater [27]. In this study, the forecasted flood depth over 0.3 m was considered a flooding cell. This criterion ensures that the models can identify the highest flood potential locations. In addition, to better demonstrate the performance of this model, the fit indicators at different thresholds of flood depth were also evaluated.

4. Results and Discussion

Figures 6–10 present the comparisons of the SPM_D (left) and SPM_E (right) for the three towns. In these figures, the flooding areas simulated from the SPM and WASH123D are “light blue” and “green”, respectively. SPM_D and SPM_E represent the SPM with the D-infinity approach and the lowest elevation approach, respectively. The overlapping flood areas and observations are “red” and “light yellow”. The purple dots are route starting cells where floods originate. Figure 11 presents the comparison of the model performance for various thresholds. For example, the grey line identifies that the performance for a threshold = 0.3 m and the cells with water depth above the threshold were treated as flooded cells. Chen *et al.* [19] described that the thresholds were chosen based on experimental values. Ishigaki *et al.* [28] suggested that inundation depth = 0.3 m is the safety limit for elders to walk through. Hereafter this study evaluates the model performance using a threshold = 0.3 m. When comparing the results in Pingtung (Figure 6), the SPM_D (0.33) has better fit indicators than the SPM_E (0.16) (Figure 11). The performance increases by 106%.

Figure 7 shows the comparison with observations. The SPM_D provided a better comparison than SPM_E in the central part of Pingtung. However, both models did not generate floods in northeastern Pingtung. It is explained by the fact that the flood occurred because of a levee failure. None of these models can forecast it at present. The comparisons in Hengchun (Figures 8 and 9) also indicate that the SPM_D outperforms the SPM_E. The fit indicators for the SPM_D and SPM_E are 0.23 and 0.12, respectively. A 91 percent increase in the performance is identified. In comparison with the observations, SPM_D was able to forecast floods in the central part of Hengchun, but SPM_E was not.

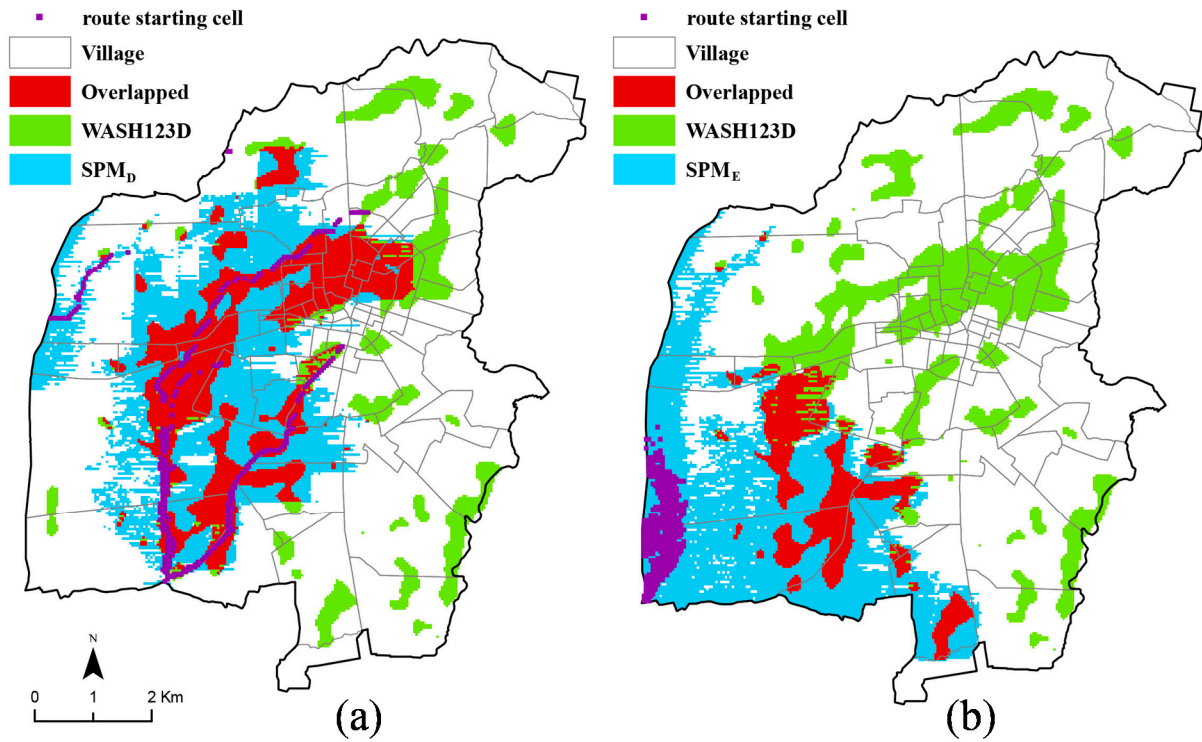


Figure 6. Overlapping flood areas at the grid level between WASH123D and SPM_D (a) and SPM_E (b) in Pingtung.

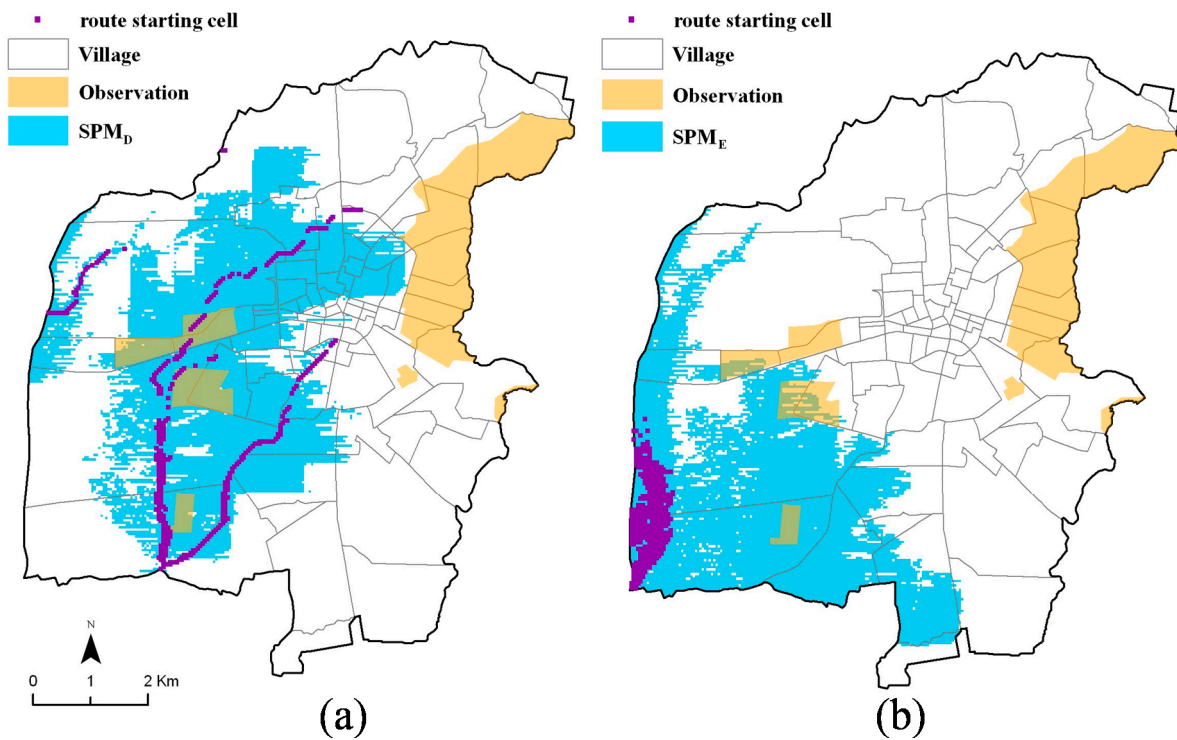


Figure 7. Overlapping flood areas at the grid level between the observed floods and SPM_D (a) and SPM_E (b) in Pingtung.

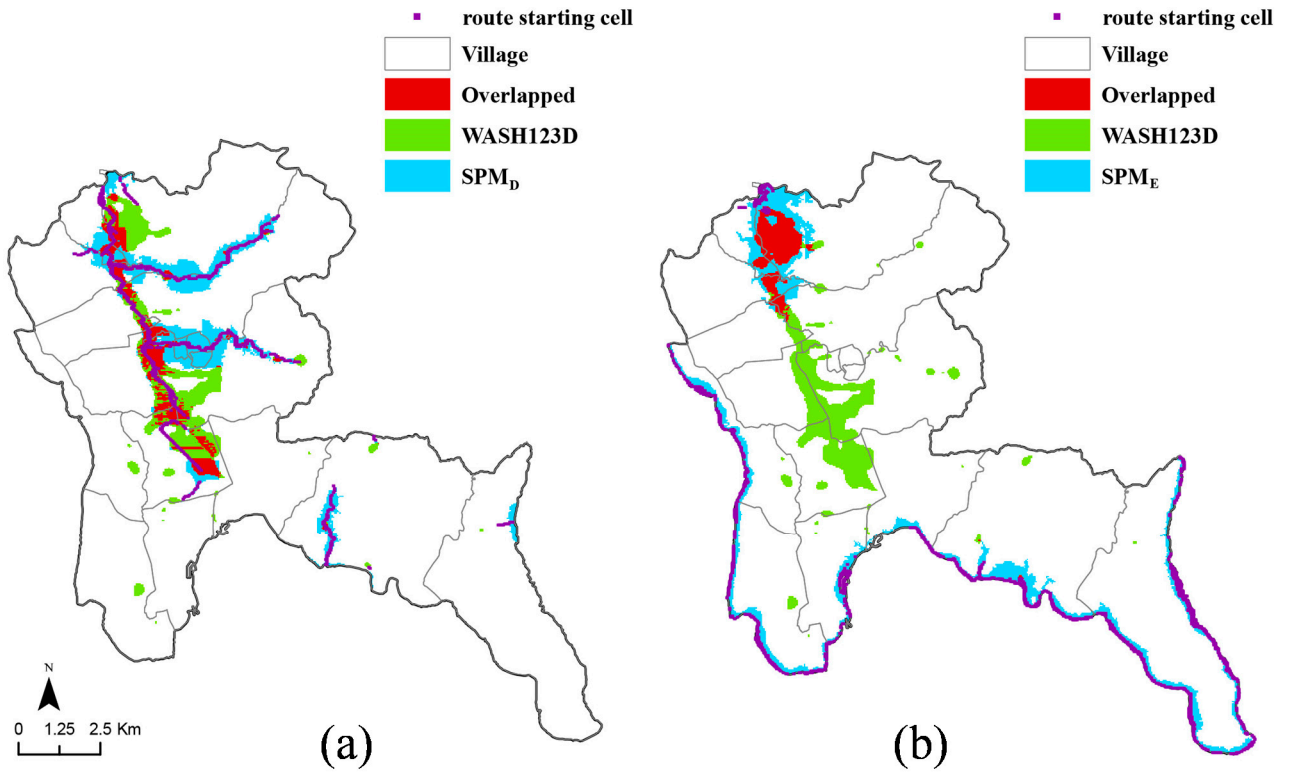


Figure 8. Overlapping flood areas at the grid level between WASH123D and SPM_D (a) and SPM_E (b) in Hengchun.

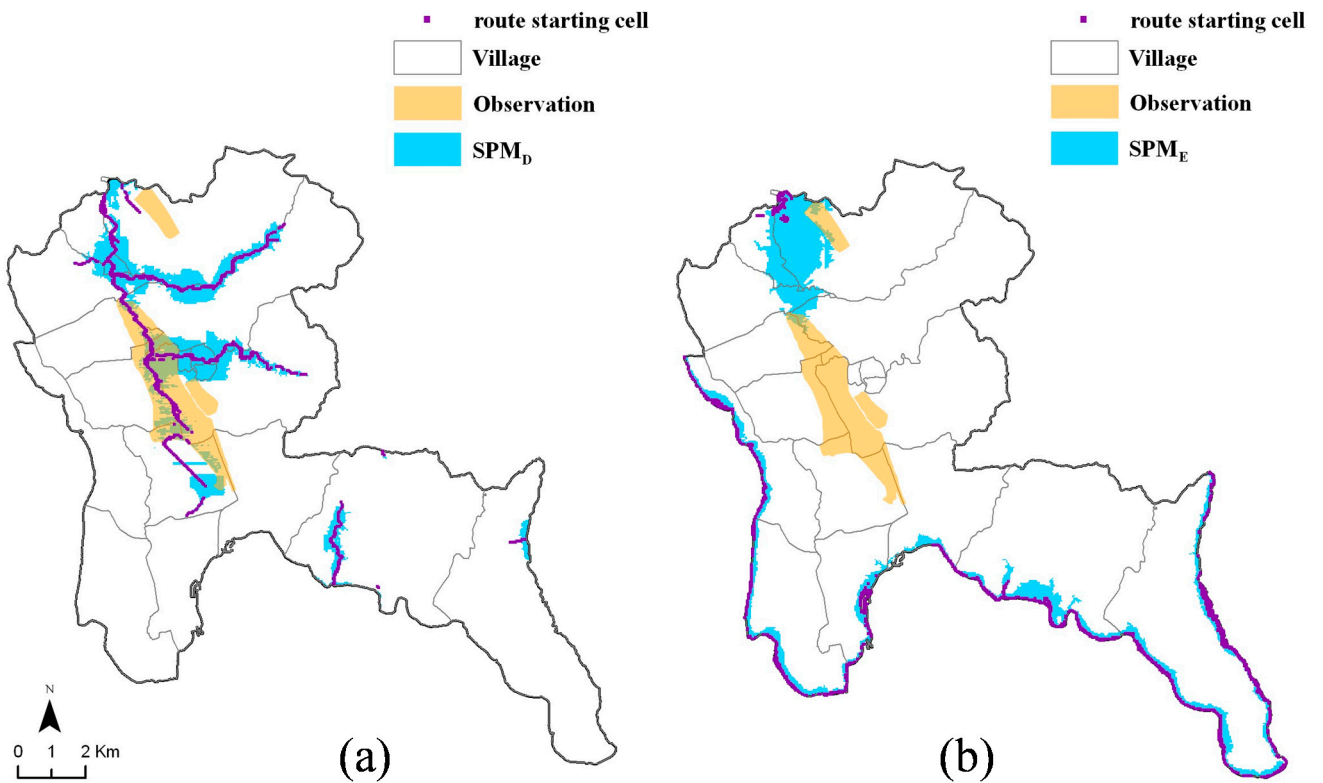


Figure 9. Overlapping flood areas at the grid level between the observed floods and SPM_D (a) and SPM_E (b) in Hengchun.

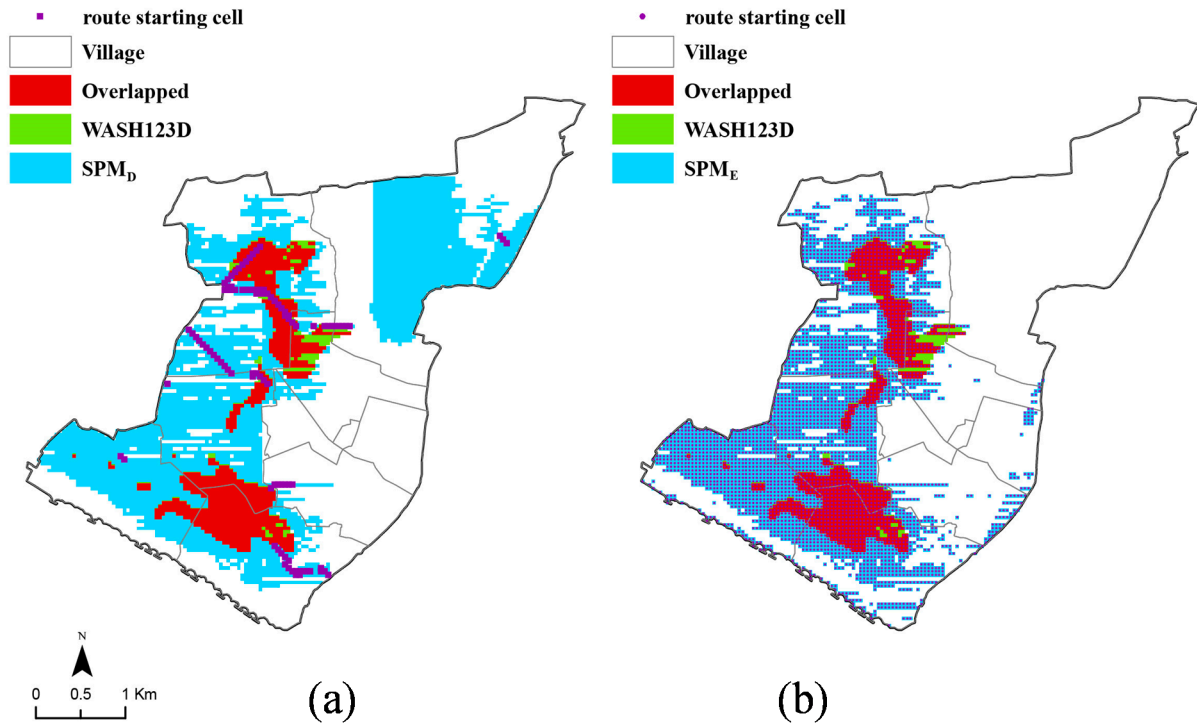


Figure 10. Overlapping flood areas at the grid level between WASH123D and SPM_D (a) and SPM_E (b) in Linbian.

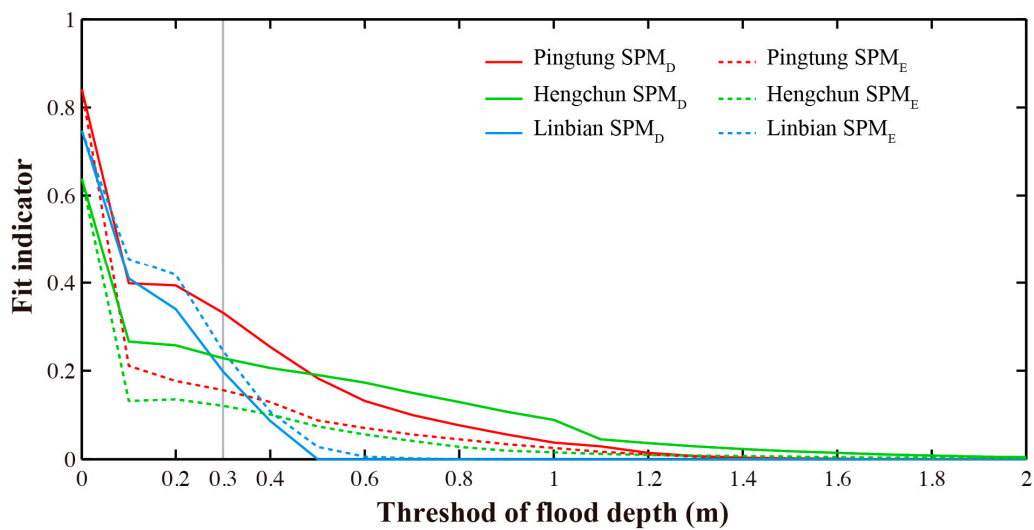


Figure 11. Comparison of the model performance between SPM_D and SPM_E using the performance indicator for various threshold values.

Figure 12 shows the model performance between SPM_D and SPM_E for various DEM resolutions. By using various DEM resolutions in Pingtung and Hengchun, the SPM_D constantly has higher fit indicators than the SPM_E. The result confirmed the above mentioned comparisons that using D-infinity approach has a better performance than using the lowest elevation. Also, Figure 12 shows that the fit indicators in Pingtung and Linbian decline with increasing DEM resolution, especially for the SPM_D. Since the SPM_D is based on the D-infinity contributing area, the resampled rough DEM loses some detailed topographical information, e.g., artificial drainage channels, which may result in rough or incorrect flow direction and

flow accumulation. In contrast, the SPM_E have similar fit indicators at different DEM resolution. This is because the resampled DEM does not change the spatial pattern of lowest elevation distinctly. The results suggest that SPM_D is more sensitive to the accuracy and resolution of a DEM than is SPM_E .

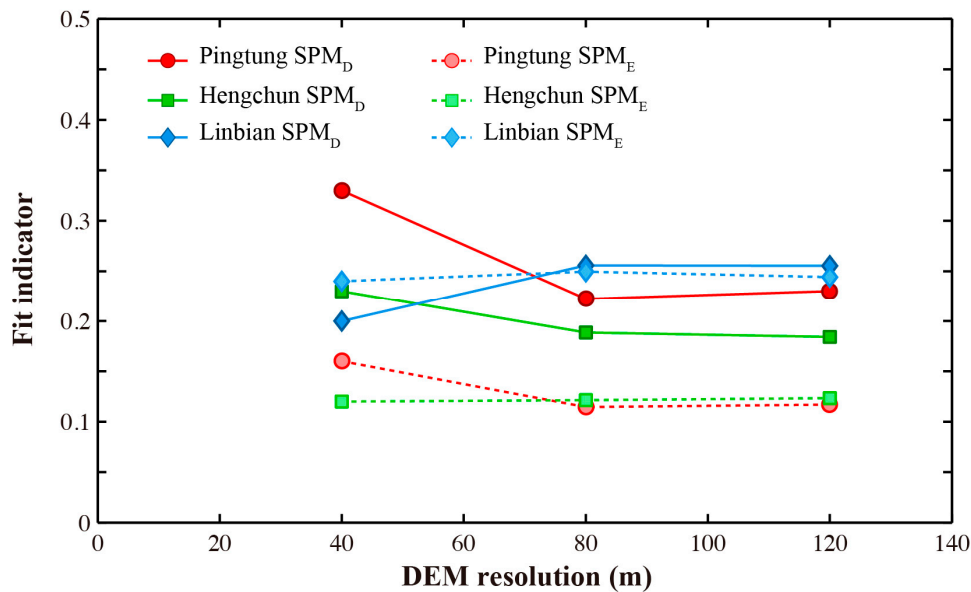


Figure 12. Comparison of the model performance between SPM_D and SPM_E using the performance indicator for various DEM resolutions.

The result of the two cases demonstrates that selecting the route starting cells is important for the flat-water model. Using the most commonly applied lowest elevation approach, the SPM_E forecasted the flood areas at relatively lower locations, which were consistent with the topographic depressions in Figure 5. Logically, the low-lying cells have a high risk of flooding. Elevation alone, however, is not sufficient to explain urban flooding with a relatively gentle slope because the flooding may also originate where high flows from a local sub-watershed occurred, depending on the selection of the route starting cells. Thus, the D-infinity contributing area approach is introduced into the flat-water model. This approach not only considers elevation but also includes accumulated water from the upstream area. The improved performance is confirmed in the above mentioned comparisons

However, the results of the comparison in Linbian are the opposite: the fit number is higher for the SPM_E than for the SPM_D , although the overlapping areas with WASH123D are similar (Figure 10). The performance of the fit indicators for the SPM_D and SPM_E are 0.20 and 0.24, respectively, decreasing by 16% for a threshold = 0.3 m (Figure 11). Previous studies (e.g., [4,19]) demonstrated that choosing the lowest elevation for the route starting cells in the flat-water assumption is appropriate in flat areas. However, Falter *et al.* [12] found a problem related to simplified flood models: isolated ponds were simulated by the infilling at the lowest point. This problem is likely to be less important in areas with a complex topography. Unfortunately, no studies (e.g., [4,12,19]) have provided the definition of a flat area. An additional problem is apparent. The results of SPM_E s (Figures 6–9) show that the flooded areas are originated from globally low-lying locations (purple points). It does not provide better forecasts in comparison with SPM_D . However, the finding is not applied to the application in the flat area. In Linbian, all of the elevations are below 10 m, and most of them range 0–2 m; thus, the area is topographically flat (Figure 5). The performances of the SPM_E and SPM_D are highly similar, as shown in Figures 10 and 11.

SPM_E selects the lowest one percent of all cells to start flooding. For Linbian, the corresponded elevation is 0 m and there are more cells with the same elevation. This study added those extra cells into routing start cells, as shown in Figure 10. The results showed that the flooded area is identical to the covered area of the routing start cells. SPM_E did not generate the flooded area at the top-right region in comparison with SPM_D. It slightly increased the performance of SPM_E.

In the present study, we were unable to determine with certainty which approach is better for particular topographies. This topic should be addressed in future SPM improvements. For more complex topography, such as that in Pingtung and Hengchun, the changes in elevation are significant, and the SPM_D performed relatively well. Despite the slight decrease in the case of Linbian, SPM_D is recommended for all topographies. In summary, SPM is currently not acceptable for use by public officials. However, this study proposed a novel idea, *i.e.*, the consideration of elevation and flow accumulation (SPM_D) instead of only elevation (SPM_E) to identify locations where flooding originates, that can be applied in a simplified inundation model.

During an emergency, rescue resources are limited and are usually collected in a central emergency response center in a large administrative area. Then, decision-makers allocate the limited resources to smaller districts according to the flooding risk. Apel *et al.* [29] suggested that simplified models offer the best spatially distributed representation of maximum inundation depths. Combined with flood loss models, simplified models are valuable for rapid flood-loss estimations. Because of the efficiency of SPM, another aspect of the model is described. Decision-makers require fast analyses to evaluate the possible flood threat or to prioritize zones with a high flood risk when multiple zones are present. In this study, a large administrative area is defined as a town, and a zone is defined as a village for which decision-makers allocate rescue resources. Using the same fit indicator in Equation (2), Table 1 presents the analysis results in terms of the overlapping flood forecasts at the village level. The SPM_D still performed better than the SPM_E. The best fit number occurred in Pingtung at 0.69 with the SPM_D, which is 0.5 higher than the number achieved with the SPM_E. All of the fit numbers of SPM_E are close to 0.7. Thus, approximately 70% of the forecasts are consistent with WASH123D at the village level. The SPM_D can provide timely information with acceptable accuracy at the village level and serve as an easy-to-use tool for decision makers to prioritize villages with a high risk of flooding.

Table 1. Comparison of overlapping villages between WASH123D, SPM_D, and SPM_E using the performance indicator.

Town	Fit Indicator	
	SPM _D	SPM _E
Pingtung	0.69	0.19
Hengchun	0.71	0.65
Linbian	0.75	0.75

5. Conclusions

The development of simplified inundation models has become popular for providing efficient forecasts. A simplified inundation model was proposed in this study based on the flat-water assumption. Selecting a collection of route starting cells is important for applying this type of simplified model. This study used two approaches to select the collection of cells from which flooding is assumed to originate: First,

the lowest elevation approach, which includes elevation as the single criterion; and second, the D-infinity contributing area approach, which is a novel approach that considers elevation, flow direction, and flow accumulation to select route starting cells. The results showed that using the D-infinity contributing-area approach can improve the performance of the simplified model in various topographical conditions. However, the improvement in very flat areas was not significant. Different topographies affect the applications of the different methods when identifying route starting cells. To improve the performance of SPM, various approaches should be used in particular topographical areas; additional details, such as frictional effects and improved hydraulic connections in the flood water spread and the capabilities of steady and unsteady flood simulations, will be of interest in future studies.

A simplified inundation model was developed for its efficiency. Based on the comparison in this study, WASH123D required an average of 10–15 min to simulate flooding based on domain sizes of 9000–85,000 cells, whereas the SPM_D required less than 2 min. The calculation time can decrease within 1 min if the flow accumulation is preprocessed. The same inputs (*i.e.*, total rainfall and the DEM) were used for the comparison. The SPM_D was approximately 5–10 times more efficient than WASH123D in terms of the calculation time. A total of 33 townships are located in Pingtung County; thus, running the SPM will ultimately save time. The SPM is relatively stable and does not exhibit problems related to numerical dispersion during urgency due to a simplified assumption of water spread and straightforward model input. However, the SPM will not be considered for practical use until its predictions are comparable to those obtained from complex inundation models. The SPM_D provides acceptable comparisons at the village level based on the comparison in this study. The model cannot provide detailed flooding information, such as the time of flood occurrence. The model does not include the drainage system just yet and provides overestimated predictions. It needs to add vertical source/sink terms (*i.e.*, drainage systems) and temporal capabilities (*i.e.*, unsteady simulation) to perform better simulation scenarios. The present model is suitable for rapid assessments when there is a lack of information, such as boundary conditions and model parameters, to run a complex inundation model. The modeling results are useful for decision makers to perceive flood risks in the area and allocate rescue resources. If there is a limited response time and a detailed simulation is needed, the model can prioritize the areas of flood risk. The operator can assign preference to high flood risk areas, where a complex inundation model can then be run. A goal for improving the SPM is to provide predictions at the cell level that are comparable to those obtained from complex models.

Acknowledgments

The inundation area data used here were kindly provided by of Yi-Lung Yeh of the Department of Civil Engineering of National Pingtung University of Science and Technology. We thank five anonymous reviewers for providing constructive comments on this manuscript. This work was supported by grants from Ministry of Science and Technology of Taiwan (MOST 103-2221-E-492-038-).

Author Contributions

Tsun-Hua Yang and Yi-Chin Chen designed and performed the model and wrote the manuscript. Ya-Chi Chang performed the WASH123D model and validated the model performance. Sheng-Chi

Yang and Jui-Yi Ho analyzed data and modified the paper. All authors discussed the results and implications and commented on the manuscript at all stages.

Conflicts of Interest

The authors declare no conflict of interest.

References

1. Evans, E.P.; Ashley, R.; Hall, J.; Penning-Rowsell, E.; Saul, A.; Sayers, P.; Thorne, C.; Watkinson, A. *Foresight Flood and Coastal Defense Project: Scientific Summary: Volume I, Future Risks and Their Drivers*; Office of Science and Technology: London, UK, 2004.
2. Choi, S.; Choi, S.Y.; Kim, K. Study on the development of the loss estimation method for urban flood in Korea. In *Disaster Management and Human Health Risk III: Reducing Risk, Improving Outcomes*; Brebbia, C.A., Ed.; Wessex Institute of Technology: Southampton, UK, 2013; Volume 133, p. 11151.
3. LaRocque, L.A.; Elkholy, M.; Hanif-Chaudhry, M.; Imran, J. Experiments on urban flooding caused by a levee breach. *J. Hydraul. Eng.* **2013**, *139*, 960–973.
4. Zerger, A.; Smith, D.I.; Hunter, G.J.; Jones, S.D. Riding the storm: A comparison of uncertainty modeling techniques for storm surge risk management. *Appl. Geogr.* **2002**, *22*, 307–330.
5. Prestinzi, P. Suitability of the diffusive model for dam break simulation: Application to a CADAM experiment. *J. Hydraul. Eng.* **2008**, *361*, 172–185.
6. Bates, P.D.; de Roo, A.P.J. A simple raster-based model for flood inundation simulation. *J. Hydrol.* **2000**, *236*, 54–77.
7. Lhomme, J.; Sayers, P.B.; Gouldby, B.P.; Samuels, P.G.; Wills, M.; Mulet-Marti, J. Recent development and application of a rapid flood spreading method. In *Proceedings of the Flood Risk 2008 Conference*, Oxford, UK, 30 September–2 October 2008; Taylor and Francis Group: London, UK, 2008.
8. Krupka, M. A Rapid Inundation Flood Cell Model for Flood Risk Analysis. Ph.D. Thesis, Heriot-Watt University, Edinburgh, Scotland, 2009.
9. Liu, Y.; Pender, G. A new rapid flood inundation model. In *Proceedings of the first IAHR European Congress*, Edinburgh, Scotland, UK, 4–6 May 2010.
10. Ballinger, J.; Jackson, B.; Pechlivanidis, I.; Ries, W. *Potential Flooding and Inundation on the Hutt River*; School of Geography, the Environment, and Earth Sciences, Victoria University of Wellington: Wellington, New Zealand, 2011.
11. Bernini, A.; Franchini, M. A rapid model for delimiting flooded areas. *Water Resour. Manag.* **2013**, *27*, 3825–3846.
12. Falter, D.; Vorogushyn, S.; Lhomme, J.; Apel, H.; Gouldby, B.; Merz, B. Hydraulic model evaluation for large-scale flood risk assessments. *Hydrol. Process.* **2013**, *27*, 1331–1340.
13. Shih, D.; Yeh, G. Identified model parameterization, calibration, and validation of the physically distributed hydrological model WASH123D in Taiwan. *J. Hydraul. Eng.* **2011**, *16*, 126–136.
14. Shih, D.; Chen, C.H.; Yeh, G. Improving our understanding of flood forecasting using earlier hydro-meteorological intelligence. *J. Hydrol.* **2014**, *512*, 470–481.

15. O'Brien, J.S.; Julien, P.Y.; Fullerton, W.T. Two-Dimensional water flood and mudflow simulation. *J. Hydraul. Eng.* **1993**, *119*, 244–261.
16. Lamb, R.; Crossley, M.; Waller, S. A fast two-dimensional floodplain inundation model. *Proc. Inst. Civil Eng. Water Manag.* **2009**, *162*, 363–370.
17. Kalyanapu, A.; Shankar, S.; Pardyjak, E.R.; Judi, D.R.; Burian, S.J. Assessment of GPU computational enhancement to a 2-D flood model. *Environ. Model. Softw.* **2011**, *26*, 1009–1016.
18. Smith, L.S.; Liang, Q.H.; Quinn, P.F. Towards a hydrodynamic modelling framework appropriate for applications in urban flood assessment and mitigation using heterogeneous computing. *Urban Water J.* **2015**, *12*, 67–78.
19. Chen, J.; Hill, A.A.; Urbano, L.D. A gis-based model for urban flood inundation. *J. Hydrol.* **2009**, *373*, 184–192.
20. Soulis, K.X. Development of a simplified grid cells ordering method facilitating GIS-based spatially distributed hydrological modeling. *Comput. Geosci.* **2013**, *54*, 160–163.
21. Tarboton, D.G. A new method for the determination of flow directions and upslope areas in grid digital elevation models. *Water Resour. Res.* **1997**, *33*, 309–319.
22. Jenson, S.K.; Domingue, J.O. Extracting topographic structure from digital elevation data for geographic information system analysis. *Photogramm. Eng. Remote Sens.* **1988**, *54*, 1593–1600.
23. Barnes, R.; Lehman, C.; Mulla, D. Priority-Flood: An optimal depression-filling and watershed-labeling algorithm for digital elevation models. *Comput. Geosci.* **2014**, *62*, 117–127.
24. Blanc, J.; Hall, J.W.; Roche, N.; Dawson, R.J.; Cesses, Y.; Burton, A.; Kilsby, C.G. Enhanced efficiency of pluvial flood risk estimation in urban areas using spatial-temporal rainfall simulations. *J. Flood Risk Manag.* **2012**, *5*, 143–152.
25. Yeh, G.T.; Huang, G.B.; Zhang, F.; Cheng, H.P.; Lin, H.C. *WASH123D: A Numerical Model of Flow, Thermal Transport, and Salinity, Sediment, and Water Quality Transport in WaterShed Systems of 1-D Stream-River Network, 2-D Overland Regime, and 3-D Subsurface Media*; A Technical Report; Department of Civil and Environmental Engineering, University of Central Florida: Orlando, FL, USA, 2006.
26. Yeh, G.T.; Shih, D.S.; Cheng, J.C. An integrated media, integrated processes watershed model. *Comput. Fluids* **2011**, *45*, 2–13.
27. *Risk of Flooding from Surface Water: Understanding and Using the Map*; Environment Agency: Rotherham, UK, 2010.
28. Ishigaki, T.; Kawanaka, R.; Onishi, Y.; Shimada, H.; Toda, K.; Baba, Y. Assessment of safety on evacuating route during underground flooding. *Adv. Water Resour. Hydraul. Eng.* **2009**, 141–146, doi:10.1007/978-3-540-89465-0_27.
29. Apel, H.; Aronica, G.T.; Kreibich, H.; Thielen, A.H. Flood risk analyses-how detailed do we need to be? *Nat. Hazards* **2009**, *49*, 79–98.